On the Formation Enthalpies and Bandgaps of Linear, Cyclic and Cubic Neutral Sodium Chloride Clusters $(NaCl)_n$, n = 2, 3, 4, 5, 6, 10

Samantha C. Jasinski, Constantinos D. Zeinalipour-Yazdi*

Department of Chemistry, University of East London, Stratford Campus, Water Lane, London E15 4LZ, UK

*Correspondence to: c.zeinalipour-yazdi@uel.ac.uk and zeinalip@gmail.com

Abstract

We have taken a detailed molecular mechanics and DFT investigation of various linear, cyclic, cubic 2D and cubic 3D structures of neutral sodium chloride clusters. Our results explain the stability of these structures and calculate the lattice formation enthalpy and the bandgaps of these structures. We find that linear chains of NaCl clusters have a significantly smaller bandgap than cyclic and cubic clusters. This may find use in the use of new NaCl clusters geometries for applications in photovoltaics and high-speed infrared induced electronics.

Keywords: NaCl, clusters, DFT, cyclic, linear, cubic, Sodium chloride, bandgap

1. Introduction

Sea salt aerosols are among the most important forms of salt nanoclusters found in nature and have therefore been the source of several computational investigations.[1,2] These nanoclusters from the evaporation of seawater droplets.[3] A better understanding of NaCl cluster formation may improve models for cloud formation and climate change.[4,5] It is evident that the structure and stability of small neutral and charged sodium chloride clusters is considerably different than that of the macroscopic cubic crystal lattice and therefore this topic has been the main focus of many computational and experimental studies.[6-12] Alkali halide clusters can be studied in supersonic expansions using mass spectrometers with numerous applications from catalysis to new cluster-assembled materials.[13] Understanding the nucleation process in alkali metal chlorides has been the focus of many experimental studies using electrospray ionization, UV-laser and magnetron-sputter sources coupled to mass spectrometry.[14-16]

The mechanical properties, the structural transitions, and the global minima of sodium chloride clusters have been thoroughly investigated by interatomic potentials by Doye and Wales.[17,18] A genetic algorithm was used to explore the potential energy surface of sodium chloride clusters with up to 100 ions and found that the global minimum is a cubic lattice.[19] A study of inter-atomic potentials showed that the potentials and fields of salt crystals can be classified into corner, edge, face, and interior potentials.[20] The relative stability and cohesive energy of sodium chloride nanotubes have been studied via DFT Baker et *al*. and it was found that increasing the length and decreasing the widths of nanotubes results in higher ionic character.[21]

There have also been many studies concerning the solvation of sodium chloride in water as this has been the textbook example for the solvation of ionic crystals. The interaction of water adlayers with the NaCl (001) surface has been studied in detail in a review article by Ewing.[22] One of the earliest studies of the water adlayer formation on NaCl (001) surfaces was done via transmission electron microscopy (TEM).[23] There are also many studies that have investigated the interaction of water with small sodium chloride clusters. The initial hydration process of positively charged sodium chloride clusters was studied with the use of mass spectrometry and DFT calculations by Bradshaw et *al*.[24] Michaelides et *al*. studied via *ab initio* molecular dynamics the hydration process of NaCl surfaces.[25,26] The sodium chloride cluster formation process was modeled via molecular dynamics to find

whether it proceeds through a charged residue model (CRM) or an ion evaporation model (IEM) and the former was found to explain the computational data.[27]

In this study we investigate the size-dependent trends of the lattice formation enthalpy, the Gibbs free lattice formation energy, the HOMO-LUMO bandgap, and the partial charges on the atoms in $(NaCl)_n$ clusters where n = 2, 3, 4, 5, 6, and 10.

2. Computational Methods

All sodium chloride cluster structures were designed in Avogadro and optimised using various starting structure using the MMFF94 force field.[28] The optimisation algorithm used was a steepest descent algorithm with a convergence criterion of 10^{-7} kJ/mol. The optimised structures from the MMFF94 calculations were then used as starting structures for DFT full optimisations within Gaussian 16W with the use of Becke's three-parameter hybrid exchange functional[29] (XC) combined with the Lee-Yang-Parr non-local correlation functional[30], abbreviated as B3LYP. The basis set that was used was Pople's 6-31G basis set with one set of diffuse functions denoted as 6-31G(d).[31,32] Linear dependencies of the basis functions were removed by using the spherical version (5d and 7f) of this basis set. The self-consistent field (SCF) convergence criteria for the root mean square (rms) density matrix and the total energy were set to 10^{-8} Hartree/bohr and 10^{-6} Hartrees, respectively.

The formation enthalpies of the various clusters were calculated for the following reaction

$$n{\cdot}Na^+(g) + n{\cdot}Cl^-(g) \rightarrow (NaCl)_n\,(g) \quad (1)$$

with the following equation,

$$\Delta_f H^{298} = (H(NaCl)_n - n(H(Na^+) + H(Cl^-)))/n \quad (2)$$

where $H(NaCl)_n$ is the enthalpy of the sodium chloride cluster in gas phase at the B3LYP/6-31G(d)(5d, 7f) level of theory, $H(Na^+)$ is the enthalpy of sodium cations in gas phase, $H(Cl^-)$ is the enthalpy of chloride ions in gas phase and n is the number of NaCl-units in the cluster. This yielded for a $(NaCl)_{16}$ cluster a lattice formation enthalpy of -771.726 kJ mol^{-1} which was within 1.95 %error of the experimental lattice formation enthalpy of -787 kJ mol^{-1} calculated using the relationship,

$$\%error = \frac{|\Delta_f H_{exp} - \Delta_f H_{calc}|}{|(\Delta_f H_{exp} + \Delta_f H_{calc})/2|} \cdot 100\% \quad (3).$$

This result indicates that the level of theory (i.e. B3LYP/6-31G(d)) used is sufficient to yield results for the formation enthalpies that are within 2% of the experimental values.

Vibrational frequencies were calculated with the harmonic oscillator approximation by diagonilizing the Hessian matrix. The infrared intensities were calculated by the following equation,

$$\left[\int \psi_{v=0} \frac{\partial \boldsymbol{\mu}}{\partial q_i} \psi_{v=1} dq_i\right]^2 \quad (4),$$

where the dipole derivatives are calculated analytically[33] from the optimised structures are B3LYP/6-31G(d) with a spherical expansion of the basis (5d 7f).

Partial charges and population analysis were performed with the atomic polar tensor (APT) method.[34]

3. Results and Discussion

3.1 Force field optimizations of cyclic sodium chloride cluster using MMFF94

Investigation of how the energetic and structural parameters of NaCl clusters change is important in understanding the structure and stability of such clusters. We have used molecular mechanics calculations to see whether there is a trend in cyclic $(NaCl)_n$ clusters where n = 1 to n = 10. The results of these calculations are shown in Fig. 1 which plots the binding energy of the cyclic $(NaCl)_n$ as a function of the number of Na-Cl units in the cluster.

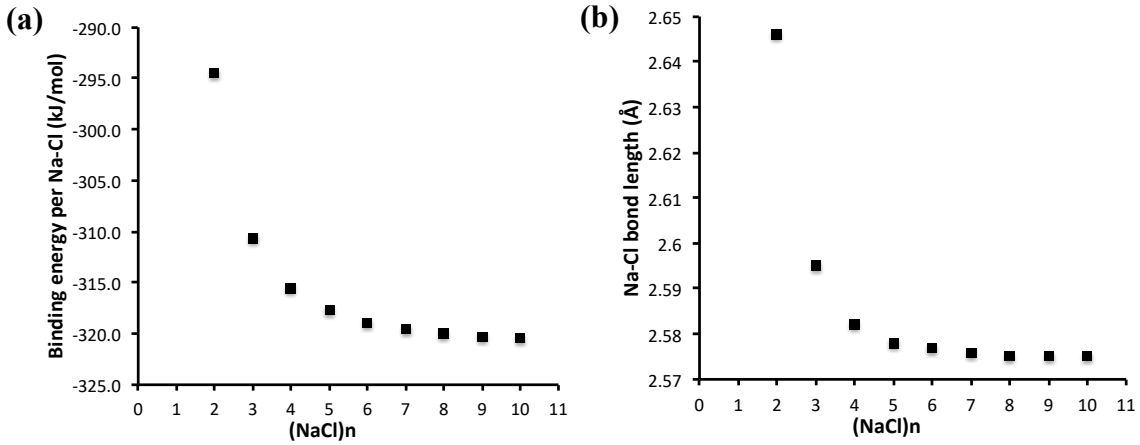

Fig. 1. (a) Binding energy per Na-Cl unit and (b) Na-Cl bond length for cyclic $(NaCl)_n$ clusters as a function of cluster size (n) using the MMFF94 force field.

Fig. 1a shows a nice converging trend of the binding energy per Na-Cl unit as a function of the number (n) of Na-Cl units. For $(NaCl)_{10}$ the binding energy has converged to 0.2 kJ mol^{-1} and further increase of the nanocluster radius does not have an effect on the binding energies per Na-Cl unit.

In Fig. 1b we show how the Na-Cl bond length changes as a function of Na-Cl units in the cyclic nanocluster. One can clearly see that the converging trend of the Na-Cl bond length (Fig. 1b) is much faster than that of the binding energy per Na-Cl unit (Fig. 1a). In particular, for this graph (i.e. Fig. 1b) even for n = 7 the bond length has converged to 0.001 Å whereas it is required to go as far as n = 10 to see a convergence of the binding energy per Na-Cl unit. This suggests that structural parameters converge much faster than energetic parameters each at the MMFF94 level of theory. These computationally inexpensive results suggested to us that we can explore the size-dependent trends of physical parameters in $(NaCl)_n$ clusters where $n < 10$ and get relatively good convergence of the physical parameters explored. As there is little confidence one can place in the energies calculated with the MMFF94 force field we undertake density functional theory (DFT) calculations.

3.2 DFT optimisations of $(NaCl)_n$ clusters where n = 2, 3, 4, 5, 6 and 10

The initial structure for the B3LYP/6-31G(d) optimisations of the various neutral sodium chloride clusters with the general formula $(NaCl)_n$ (where n = 2, 3, 4, 5, 6, 10) was obtained from a computationally inexpensive MMFF94 force field optimisations. For the MMFF94 optimisations we were able to explore a large number of conformations by manipulating the structures while the cluster was becoming optimised. This is a unique feature of the Avogadro software which makes the exploration of the potential energy surface possible by real-time intervention of the user to guide the calculation towards the desired structure that maybe higher in energy. These manipulations could clearly identify the structures that were local minima on the potential energy surface of the clusters. This allowed the finding of certain high-energy structures of the sodium chloride cluster such as the linear and cyclic structures along with the cubic that are shown in Fig. 2. And are in agreement with earlier ab initio studies.[9,11]

Since the energy differences between the various structural isomers of sodium chloride had the correct trend but the absolute value of the energy seemed to be

overestimated by the force field method we only report the B3LYP/6-31G(d) results from this point forward.

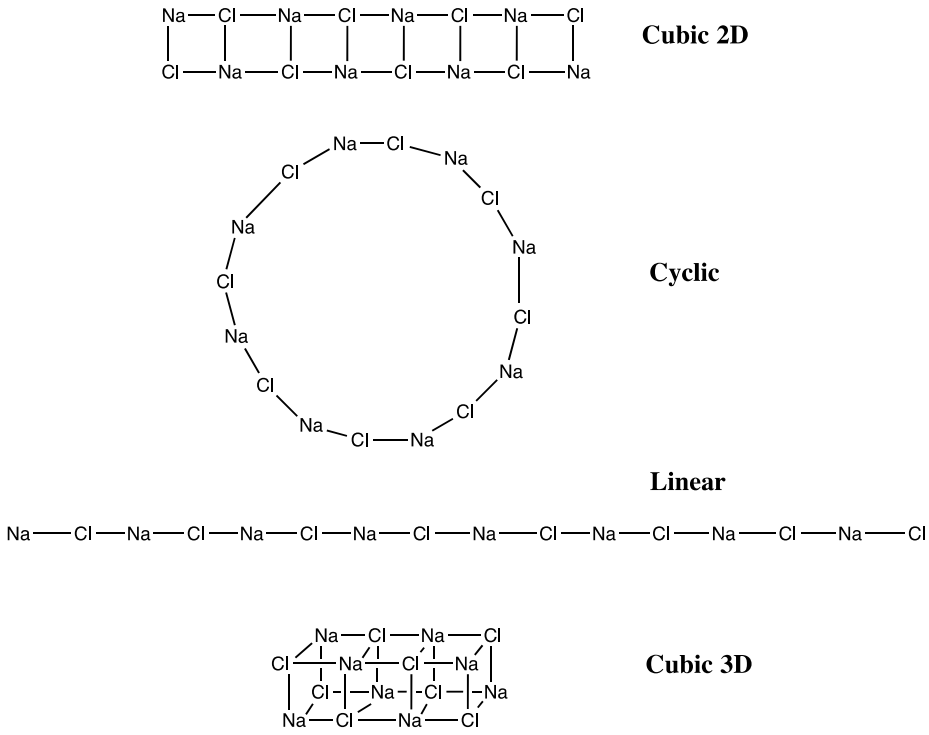

Fig. 2. Various $(NaCl)_8$ clusters that have cubic 2D, cyclic, linear, and cubic 3D structures.

3.3 Lattice formation enthalpy and Gibbs free energy of various NaCl clusters

The lattice fomation enthalpy in crystals indicates the strength of the interaction between cations and anions. It is also correlated to the thermal stability of crystallic compounds. In this section we investigate the trends of lattice formation enthalpies and the formation Gibbs free energies for NaCl clusters that have certain high symmetry geometries. These DFT calculations reveal the relative stability of the various NaCl formations and explain why large crystals of NaCl prefer to arrange in cubic 3D array rather than linear or even cyclic configurations. The search method that we used to get the initial structure for DFT optimisations was a molecular mechanics approach, which was coupled to the human interventions of leading the cluster optimisation into higher energy local minima on the potential energy surface. Such an approach to the best of our knowledge has not been previously employed in the search of the potential energy surface of small clusters. This approach indeed results in well defined arrangements of $(NaCl)_n$ that have either cubic 3D, cubic 2D,

cyclic and linear geometries as shown in Fig. 2 for $(NaCl)_8$. These higher energy structures have not been previously considered in detail by previous studies but we show that they are possible on the basis of thermodynamic properties such as the lattice fomation enthalpy (Δ_fH^{298}) and the Gibbs free energy of lattice formation (Δ_fG^{298}).

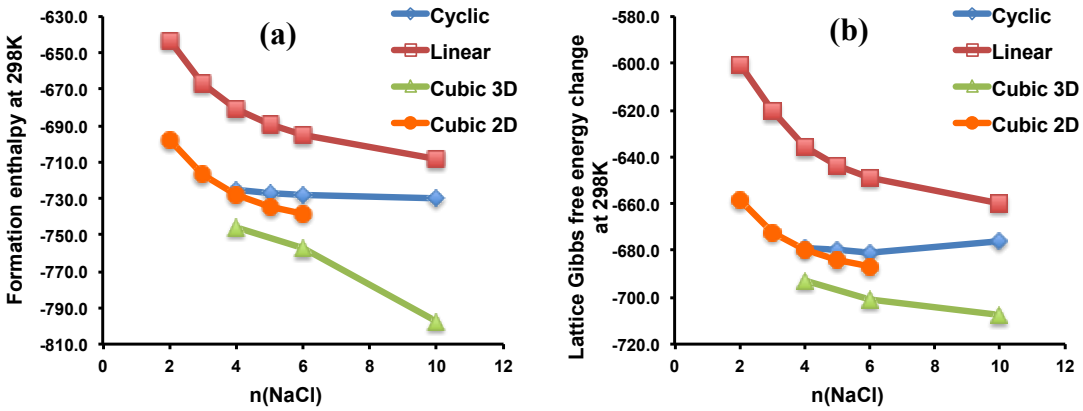

Fig. 3 (a) Lattice formation enthalpy at 298K (Δ_fH^{298}) and (b) Gibbs free energy (Δ_fG^{298}) of lattice formation for cubic 3D, cubic 2D, cyclic and linear neutral sodium chloride clusters.

In Fig. 3 we show the lattice formation enthalpy (Δ_fH^{298}) and the Gibbs free energy of lattice formation (Δ_fG^{298}) change as a function of the number of NaCl units in the cluster. In red the linear structure had the least exothermic lattice formation enthalpy (Δ_fH^{298}) and Gibbs free energy of lattice formation (Δ_fG^{298}) which converges to a value of -708.5 kJ mol^{-1} and -659.8 kJ mol^{-1}, respectively, for n=10. These values suggest that the linear structure is the least stable and requires a smaller amount of heat to form Na+ and Cl- ions. Following in stability is the cyclic structure which has lattice formation enthalpies (Δ_fH^{298}) and the Gibbs free energy of lattice formation (Δ_fG^{298}) similar to the cubic 2D structure, although the latter is to a small degree more stable. The most stable structure and the one that has the most negative lattice formation enthalpy (Δ_fH^{298}) and the Gibbs free energy of lattice formation (Δ_fG^{298}) is the cubic 3D structure. The value of the lattice formation enthalpy for n=10 is equal to -797.3 kJ mol^{-1} which is close to the experimental lattice formation enthalpy (i.e. -787 kJ mol^{-1}). This thermodynamic property does not seem to be converging even for n = 10 which may suggest that there may be a linear cubic 3D structures of NaCl (like needles) that have greater stability of the full 3D cubic arrangement of the crystal.

This is in agreement with needle-like formation of NaCl crystals that have been previously observed experimentally[35,36]. Furthermore, the higher stability of the «cuboid-like» structures has been previously addressed by *ab initio* and interatomic potential calculations on nonstoichiometric $[(NaI)_nNa]^+$ (n<~14) and $[(NaCl)_nNa]^+$ (n<18) cluster ions, respectively.[37,38] Linear and cyclic formations of negatively charged NaCl dimers have been previously calculated by *ab initio* and explained in which orbital the additional negative charge is kept.[39]

3.4 HOMO-LUMO gap in various NaCl clusters

The HOMO-LUMO gap in crystals is the energy difference between a molecule's Highest Occupied Molecular Orbital (HOMO) and its Lowest Unoccupied Molecular Orbital (LUMO). It can give an indication of how easily a material is photoexcited or how reactive a material is. It can also yield information about the electronic properties of a material, whether it is conductive, has semiconducting properties, or is a large bandgap material. In this section, we investigate the HOMO-LUMO gap in the NaCl clusters optimised in the previous section. Fig. 4 shows the HOMO-LUMO gap in $(NaCl)_n$ clusters where n = 2, 3, 4, 5, 6, and 10.

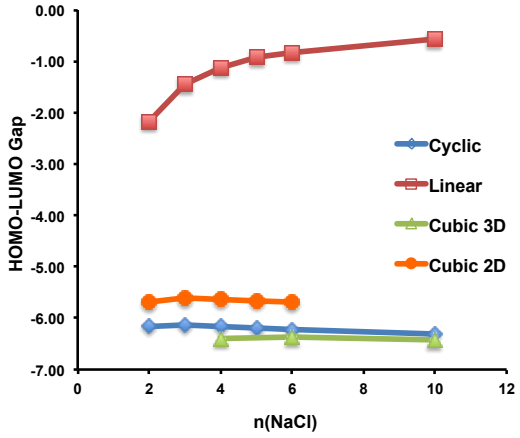

Fig. 4 HOMO-LUMO gap in cubic 3D, cubic 2D, cyclic, and linear neutral sodium chloride clusters

The HOMO-LUMO gaps are the largest for the cubic 3D NaCl clusters (6.19 eV), followed by the cyclic strutures (6.20 eV), followed by the Cubic 2D structures (5.65 eV). This bandgap corresponds to the wavelength range 194 nm to 219 nm

which is in the UV region of the electromagnetic spectrum. The smallest HOMO-LUMO gap is observed in the linear NaCl clusters and it is surprisingly different than the rest of the structures. In particular, it shows a converging trend towards a zero-bandgap semiconductor as the size of the linear chan increases. The linear NaCl clusters appear to have the unusual property that their bandgap can be tailored between 2.18 eV and 0.57 eV for n = 2 and n = 10, respectively. This suggests that small linear chains of sodium chloride can absorb photon wavelength in the range of 570 nm (visible) to 2170 nm (infrared), which corresponds to the absorption of visible and infrared light. One could think of numerous applications where this could find use such as photovoltaics and high-speed infrared induced electronics since sodium chloride doped in tin oxide has previously been shown to enhance the performance and electron transport properties of perovskite solar cells.[40]

3.4 Gibbs free energy per NaCl unit

The Gibbs free energy per NaCl unit (i.e. G/n) can determine the relative thermodynamic stability of the NaCl clusters. The trends look very similar to the lattice formation Gibbs free energy calculated in section 3.3 but are provided again in order to show the absolute value of the energetic difference of the various clusters having considered zero-point-energy (ZPE) corrections of the energies.

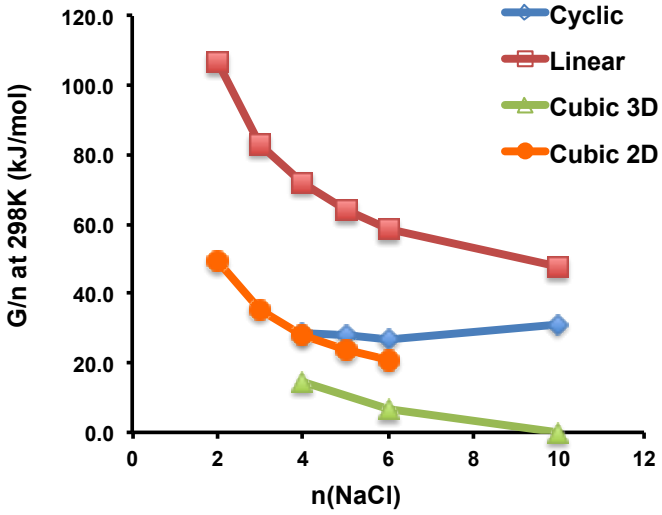

Fig. 5 Relative Gibbs free energy per NaCl unit in cubic 3D, cubic 2D, cyclic, and linear neutral sodium chloride clusters

We observe a similar ordering of the relative stability of the various NaCl clusters like the one calculated for the lattice formation Gibbs free energies. In particular, at n = 6 the cubic 3D cluster has a G/n that has a value of 6.6 kJ mol^{-1}. This structure is the most stable for the sodium clusters investigated. Next in stability is the cubic 2D clusters which have a relative G/n of 20.9 kJ mol^{-1}. Next in stability is the cyclic cluster which has a relative G/n of 26.7 kJ mol^{-1}. The least stable structure of the NaCl cluster investigated is the linear structure with a relative G/n that is 58.5 kJ mol^{-1}. These results suggest that the various NaCl cluster presented have considerably different Gibbs free energies and therefore their structures are not accessible by solely thermal fluctuation at ambient temperature of 298K where the thermal fluctuations are of the order of RT = 2.4 kJ mol^{-1}. It also suggests that the growth of the higher energy (e.g. cyclic and linear) structure can only be a result of kinetic reasons. It is noted long line structures of NaCl have been grown on mica along with cubic and trigonal arrays and imaged via atomic force microscopy (AFM).[41] We, therefore, suggest that efforts should be made to see whether cyclic structures as the ones modeled here can be imaged on substrates using AFM as such structures have not been previously experimentally reported.

3.5 Calculated IR spectra of $(NaCl)_6$

The IR spectra of clusters can give us information about the strength of the chemical bonds in the structure and also guide the assignment of experimental IR peaks. According to the simple harmonic oscillator model which can calculate the vibrational frequency of diatomics we know that the vibrational frequency and hence the wavenumber are proportional to the following expression,

$$\tilde{\nu} \propto \sqrt{\frac{k}{\mu}} \qquad (5),$$

where k is the bond force constant and μ the reduced mass. This force constant is in the numerator of this equation therefore increase in the wavenumber means that the force constant also increases. The larger the force constant the stronger the chemical bond is. Therefore by rationalising the relative positions of the IR peaks in the simulated IR spectra shown in Fig. 6 we can gain details about the strength of the Na-Cl bond in the various structures.

The calculated IR absorption spectra for the various $(NaCl)_6$ structures are shown in Fig. 6. There are two prominent bands in these spectra (i) the *stretching*

mode (250 cm^{-1} to 370 cm^{-1}) of the cluster, in which the Na-Cl bond length primarily elongates and contracts during the vibration and (ii) the *bending mode* (80 cm^{-1} to 140 cm^{-1}) in which the angle between the bonds changes in a periodic way. These bands are characteristic of the sodium clusters investigated and have to the best of our knowledge not been previously assigned or measured experimentally.

The stretching mode of the linear NaCl cluster had the highest wavenumber (i.e. 368 cm^{-1}). This is followed by the cyclic NaCl cluster which absorbs at 350 cm^{-1}. Lower in wavenumber is the cubic 2D structure and the lowest wavenumber of this band is observed for the cubic 3D structure at 253 cm^{-1}. These results suggest that the stretching bond length in these structures has the order of linear > cyclic > cubic 2D > cubic 3D. It also suggests that it is harder to compress the bonds in the linear and cyclic structure than it is to compress them in the cubic structures. This nicely shows that the mechanical strength of these clusters varies and that this can be directly observed through IR spectroscopy.

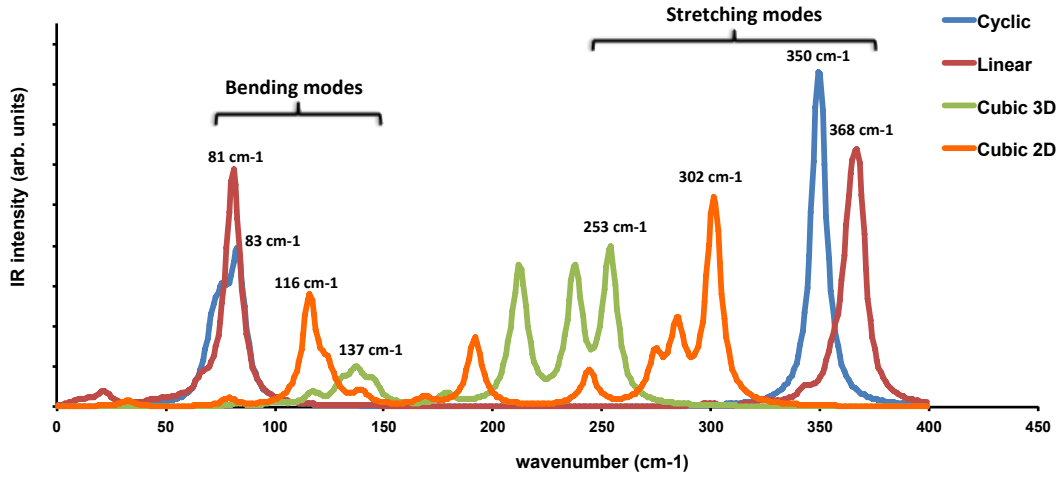

Fig. 6 Calculated IR absorption spectra of $(NaCl)_6$ for the cubic 3D, cubic 2D, cyclic and linear structures

The bending mode of these clusters follows the opposite trend of the stretching mode. In particular, we observe that the bending mode of the linear structure has now the lowest wavenumber (i.e. 81 cm^{-1}). This is means that it is easy to bend the linear NaCl structures. Slightly higher wavenumber has the bending mode of the cyclic structure but at a much lower intensity as the atoms are now somewhat confined in their bending motion to the cyclic nature of the structure. This decrease in

intensity is further intensified for the cubic 2D and the cubic 3D structures that have respectively less bending vibrations. This can be explained by the increase of the cubic lattice in the cluster, which prohibits the atoms of bending and therefore the observed intensity is less intense, of the bending mode in cubic 2D and cubic 3D. As a whole, these calculations suggest that it is easier to bend the more linear clusters than to stretch/compress them than it is to bend the cubic clusters, which are more compressible.

3.5 Calculated partial charges on Na and Cl in $(NaCl)_n$

The partial charges on atoms can give us a better understanding of the Coulombic forces that are present in an ionic cluster. These charges in the macroscopic cubic crystal of table salt are +1 for Na^+ and -1 for Cl^-. However, in small clusters of these elements, the partial charges differ from these values. So in this section, we investigate how the partial charges on the atoms change as a function of the NaCl structure.

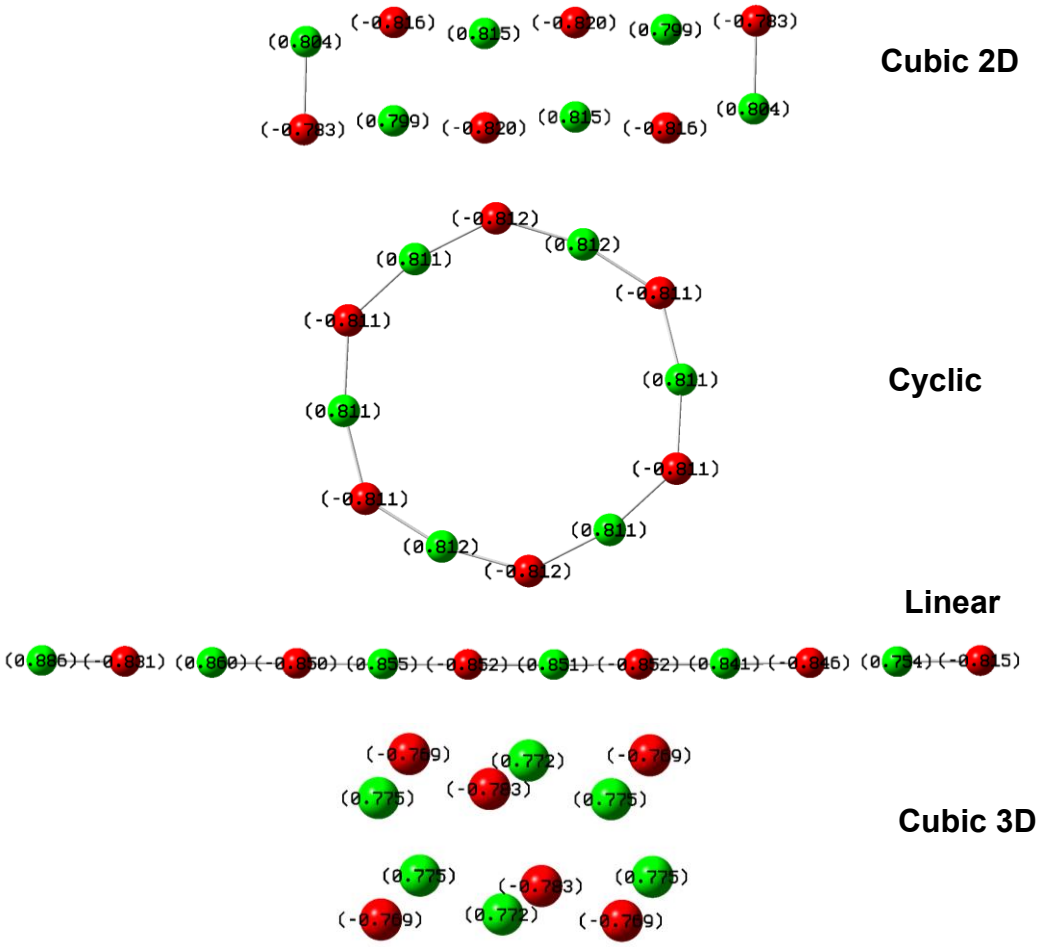

Fig. 7 Calculated ATP charges of $(NaCl)_6$ for the cubic 3D, cubic 2D, cyclic and linear structures. Sodium ions and chloride ions are shown in green and red, respectively.

The largest partial charges were observed in the linear cluster (i.e. +0.886e to -0.852e), which is in agreement with the stronger Coulombic bonds found from the simulated IR spectra. In these clusters, the charge seems to be polarised towards the side of the cluster, which has a Na atom, as the terminal atom of the chain. The charge is gradually decreasing towards the opposite side of the cluster to a value to +0.754e. This is associated with the existence of a relatively large dipole moment in this structure of 67.5 Debye. This shows that large variations of the charge of these atoms can be observed depending on the position of the atoms in the structure.

The second-largest partial charges are observed in the cubic 2D structure where the maxiumum charges are +0.815e and -0.820e for the central Na and Cl ions. This indicates that this structure has weaker Coulombic interactions compared to the

linear structure. In this cluster, the charges are greater in the center of the structure and decrease to values of +0.804e and -0.783e for Na and Cl ions, respectively, at the edges of the structure. This structure does not have a considerable dipole moment, which indicates a smaller degree of charge polarisation in the structure.

The third-largest charges are observed in the cyclic cluster where the maximum charges are +0.812e and -0.812e, respectively, for Na and Cl ions. Due to the cyclic structure of this cluster all the partial charges on the atoms are roughly equivalent. This indicates that the properties of this cluster are isotropic around the periphery and that physical and chemical properties are the same for any Na-Cl unit of the cluster. This structure does not have a considerable dipole moment.

The smallest charge separation is observed in the cubic 3D structure as the maximum partial charges range between +0.775e and -0.783e for Na and Cl ions, respectively. The lower partial charges in this structure indicate weaker Coulombic forces between the ions. The fact that the Gibbs free energy per NaCl unit is the most exothermic and indicates greater stability than the rest of the cluster might be an indication that there is also a small degree of other interactions present between the ions. This is a result of the partial charges not being exactly +1 and -1 as they are in the extended cubic lattice.

We also have investigated how the partial charges change as a function of the NaCl size. Our aim is to show that these partial charges converge to the +1 and -1 values, which are the charges the ions have in the extended NaCl lattice. In Fig. 8 we plot the positive partial charge of the sodium ion as a function of the cluster size. The data points were fitted by a logarithmic function of the form,

$$\delta^+ = aln(n) + b \tag{6}$$

where δ^+ is the partial charge on the sodium atom and n is the number of NaCl units in the cluster, whereas a and b are the fitting parameters of the logarithmic function. The equation of the fit yields a and b values 0.0407 and 0.7388, respectively, with a R-squared value of 0.99726. Solving this equation for $\delta^+ = 1$ yields a value for n = 613. This means that once the cyclic chain length is equal to 613 NaCl units the charge on the individual atoms of sodium and chloride will become +1 and -1, respectively. It reassuring to see that for large clusters the ions have the charges expected for the macroscopic crystal.

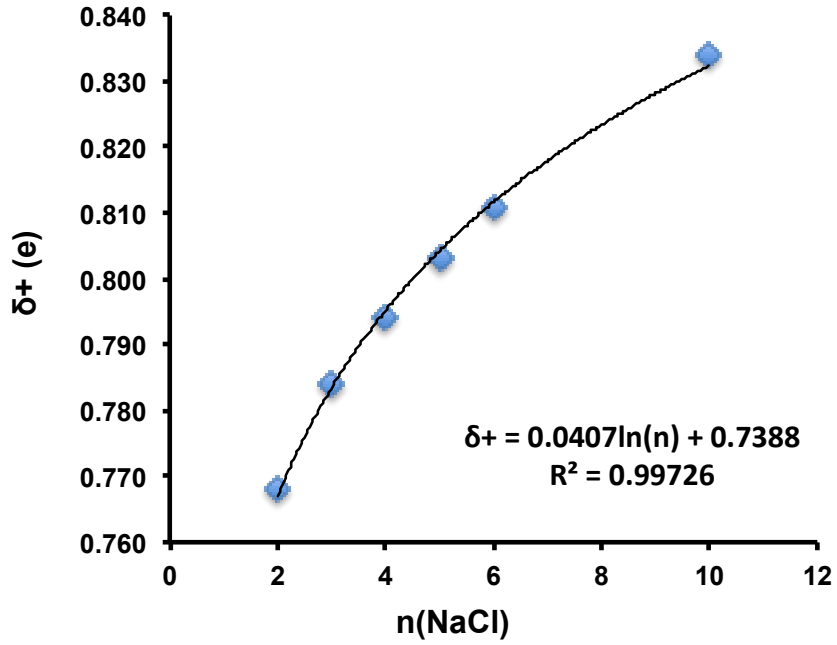

Fig. 8 Calculated ATP charges (δ^{+}) of sodium in $(NaCl)_n$ clusters for the cyclic structures as a function of cluster size.

3.6 Molecular orbitals (HOMO, LUMO) in $(NaCl)_6$ clusters

The frontier orbitals (i.e HOMO and LUMO) are mathematical functions that describe the region of space where the valence bonding and antibonding electrons are located in a cluster. They can describe how the electrons will move in a material under the influence of an external electric field. These mathematical functions are useful in understanding from where the most weakly held (i.e. by electrostatic interactions) electrons will be located and to which atoms these electrons will move upon a thermal or photo-excitation. So in this section, we investigate the size-dependent properties of the HOMO and LUMO orbitals in $(NaCl)_6$ where the structure is cubic 3D, cubic 2D, cyclic and linear.

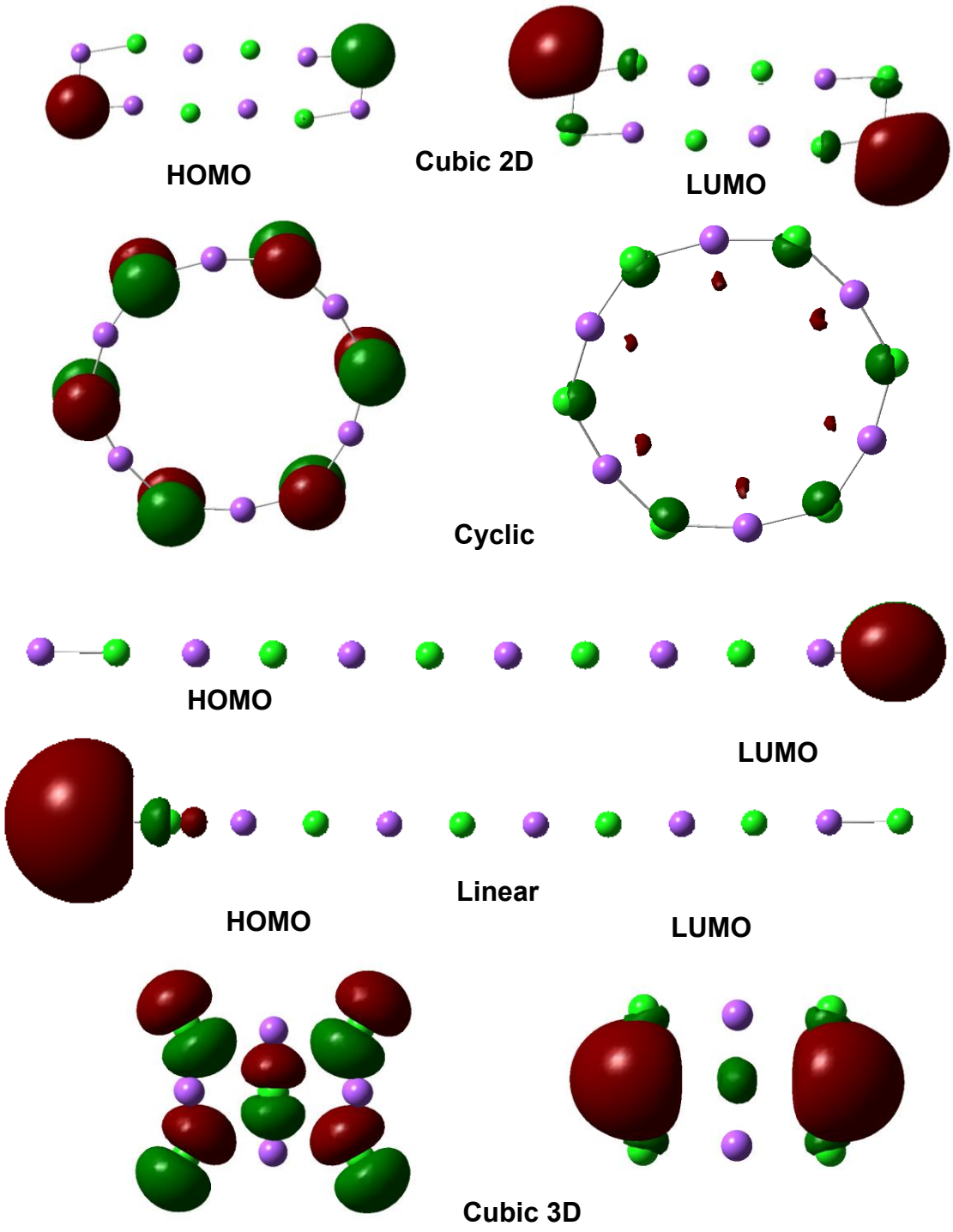

Fig. 9 HOMO and LUMO molecular orbitals of $(NaCl)_6$ clusters for the cubic 3D, cubic 2D, cyclic and linear structures. Sodium ions and chloride ions are shown in pink and green, respectively.

In Fig. 9 we present the HOMO and LUMO orbital of the various $(NaCl)_6$ clusters for the cubic 3D, cubic 2D, cyclic and linear structures. The HOMO orbitals

in all structures appear to be an orbital of p symmetry in agreement with earlier *ab initio* studies.[11] In this orbital, the lone electron pair resides which gives chloride the negative charge. In all structures, the HOMO orbital resides on the chloride. This location is either on all chloride ions, which is the case for cyclic and cubic 3D structures or it is located on just the edge chloride ion, which is the case for the linear and cubic 2D structures. It is interesting that in the linear structure the HOMO is confined to just one edge chloride ion, which is in agreement with the fact that linear NaCl chains are polarised towards the chloride edge of the structure and this is what makes this particular structure have a strong dipole moment, which was calculated in section 3.5. Furthermore, the LUMO and the HOMO orbital in the linear structures are spacially well separated being on opposing ends of the structures (see Fig. 9) We estimate that these electronic structure features of the HOMO and LUMO orbital in linear neutral NaCl clusters is what causes the bandgap to be significantly lower. These frontier orbitals are spacially well separated which allows them to become closer in energy, therefore reducing the bandgap significantly in these structures as this reduces the Pauli repulsion between electrons in the HOMO and virtually excited electrons in the LUMO. In the cubic 2D structure the HOMO orbital is on both sides of the structure on the chloride ion and therefore this structure does not develop a significant dipole moment.

The LUMO orbital in all NaCl clusters is one of σ* (i.e. sigma-antibonding) symmetry and is located always on the sodium ions which are shown in pink in Fig. 9. From the location of the HOMO and LUMO orbitals in these NaCl clusters, one can predict which clusters will have a higher probability of undergoing a thermal- or photo-induced excitation. In the cubic 2D structure both orbitals are in adjacent positions so the probability of excitation is high. However, in the linear clusters, these MOs are on opposing edges of the clusters, which indicates that a thermal- or photo-excitation has low probability. In the cyclic and cubic 3D structures these orbitals are in adjacent positions for all the atoms and therefore all atoms are expected to undergo excitations at a high probability.

Conclusions

In this molecular mechanics and DFT study, we have investigated the size-dependent trends of the lattice formation enthalpy, the Gibbs free lattice formation energy, the HOMO-LUMO bandgap, and the partial charges on the atoms in $(NaCl)_n$

clusters where n = 2, 3, 4, 5, 6 and 10. We find some interesting trends that explain the electronic structure of these clusters and how they would interact with electric fields and photons. The main results from our study are summarised here:

(i) Our DFT calculations of the Gibbs free energy per NaCl unit indicate that the most stable structure of NaCl cluster is the cubic 3D structure, followed by the cubic 2D structure, followed by the cyclic structure and the most unstable structure is the linear structure. The later structure may be the origin of needle-like formations of NaCl clusters.

(ii) For the cyclic structure, MM calculations indicate the binding energy per NaCl unit has converged to 0.2 kJ mol^{-1} for n=10 and further increase of the nanocluster radius does not have an effect on the binding energies per Na-Cl unit.

(iii) For the linear structure, we find that it has the least exothermic lattice formation enthalpy ($\Delta_f H^{298}$) and Gibbs free energy of lattice formation ($\Delta_f G^{298}$) which converges to a value of -708.5 kJ mol^{-1} and -659.8 kJ mol^{-1}, respectively, for n=10.

(iv) We find that linear chains of NaCl have a significantly smaller bandgap than cubic and cyclic structures, which suggests that they can absorb photon wavelength in the range of 570 nm (visible) to 2170 nm (infrared).

(v) Our ATP partial charge analysis indicates that small NaCl clusters have partial charges that are in the range of +/- 0.880 to +/- 0.780 which is significantly lower from the expected charge of +/- 1, but they converge to the latter charge for n = 613.

(vi) The HOMO-LUMO gaps for the cubic 3D, cyclic and cubic 2D structures are 6.19 eV, 6.20 eV, 5.65 eV, respectively. The linear NaCl clusters appear to have the unusual property that their bandgap can be tailored between 2.18 eV and 0.57 eV for n = 2 and n = 10, respectively.

(vii) Simualted IR spectra of the NaCl clusters show that there is a *stretching mode* (250 cm^{-1} to 370 cm^{-1}) and a *bending mode* (80 cm^{-1} to 140 cm^{-1}).

(viii) The HOMO orbital in NaCl clusters is of p symmetry and is located on the chloride ion whereas the LUMO orbital is of σ* symmetry and is located on the sodium ions.

(ix) Lastly, in the linear neutral NaCl clusters the frontier orbitals are spacially well separated which allows them to become closer in energy, therefore

reducing the bandgap significantly in these structures as this reduces the Pauli repulsion between electrons in the HOMO and virtually excited electrons in the LUMO, this is the origin of the reduced bandgap.

Conflicts of Interest

There are no conflicts of interest to declare

Author Statement

Constantinos D. Zeinalipour-Yazdi: Conceptualization, Methodology, Writing-Reviewing and Editing, Supervision, Samantha Jasinski: Writing- Original draft preparation, Investigation.

Acknowledgment

We would like to thank the Royal Society of Chemistry's COVID-19 Head of Department Grant (H20-134) for funding the computational resources of this work.

REFERENCES

1. Welch, D. O.*, et al.*, *J. Chem. Phys.* (1997) **68**, 2159–2171
2. Martin, T. P., *Phys. Rep.* (1983) **95**, 167–199
3. Warneck P (1988) Chemistry of the Natural Atmosphere. Academic, San Diego
4. Finlayson-Pitts, B. J., and Hemminger, J. C., *J. Phys. Chem. A* (2000) **104**, 11463
5. Finlayson-Pitts, B. J., *Chem. Rev.* (2003) **103**, 4801
6. Zhanga, S., and Chen, N., *Physica B* (2003) **325**, 172
7. Twu, Y. J.*, et al.*, *Phys. Rev. B* (1990) **42** (8), 5306
8. Dickey, R. P.*, et al.*, *J. Chem. Phys.* (1993) **98**, 2182
9. Ochsenfeld, C., and Ahlrichs, R., *J. Chem. Phys.* (1992) **97**, 3487
10. Ayuela, A.*, et al.*, *Physica B: Cond. Matt.* (1995) **212** (4), 212
11. Malliavin, M.-J., and Coudray, C., *J. Chem. Phys.* (1997) **106**, 2323
12. Aguado, A.*, et al.*, *Phys. Rev. B* (1997) **56** (23), 15353
13. Castleman, A. W., and Bowen, K. H., *J. Phys. Chem.* (1996) **100** (31), 12911
14. Wakisaka, A., *Faraday Discuss.* (2007) **136** (0), 299
15. Luo, Z.*, et al.*, *J. Phys. Chem. A* (2012) **116** (9), 2012
16. Honea, E. C.*, et al.*, *Int. J. Mass Spectrom. Ion Processes* (1990) **102**, 213
17. Doye, J. P. K., and Wales, D. J., *Phys. Rev. B* (1999) **59** (3), 2292
18. Doye, J. P. K., and Wales, D. J., *J. Chem. Phys.* (1999) **111**, 11070
19. Kabrede, H., and Hentschke, R., *J. Phys Chem. B* (2002) **106** (39), 10089
20. Fetisov, E. O.*, et al.*, *J. Phys. Chem. C* (2019) **123** (22), 14010
21. Baker, M. D.*, et al.*, *J. Phys Chem. C* (2013) **117** (48), 25742
22. Ewing G.E. (2005) H2O on NaCl: From Single Molecule, to Clusters, to Monolayer, to Thin Film, to Deliquescence. In: Wales D.J. (eds) Intermolecular

Forces and Clusters II. Structure and Bonding, vol 116. Springer, Berlin, Heidelberg. https://doi.org/10.1007/430_012
23. M, H., *et al.*, *Bull Soc Fr Mineral Crist* (1967) **90**, 320
24. Bradshaw, J. A., *et al.*, *J. Phys. Chem. A* (2012) **116** (1), 27
25. Liu, L.-M., *et al.*, *Phys. Chem. Chem. Phys.* (2011) **13** (29), 13162
26. Liu, L.-M., *et al.*, *J. Chem. Phys.* (2009) **130**, 234702
27. Konermann, L., *et al.*, *J. Phys. Chem. B* (2014) **118** (41), 12025
28. Avogadro Chemistry. (2016). Avogadro. Retrieved from http://avogadro.cc/
29. Becke, A. D., *J. Chem. Phys.* (1993) **98**, 5648
30. Lee, C., *et al.*, *Phys. Rev. B* (1988) **37**, 785
31. Ditchfield, R., *et al.*, *J. Chem. Phys.* (1971) **54**, 724
32. Hehre, W. J., *et al.*, *J. Chem. Phys.* (1972) **56**, 2257
33. McHale, J. L., *Molecular Spectroscopy*. Prentice Hall: Upper Saddle River NJ, 1999
34. Cioslowski, J., *J. Am. Chem. Soc.* (1989) **111** (22), 8333
35. Townsend, E. R., *et al.*, *Crystal Growth & Design* (2018) **18** (2), 755
36. Hinegardner, W. S., *J. Am. Chem. Soc.* (1933) **55** (4), 1461
37. Aguado, A., *et al.*, *Phys. Rev. B* (1998) **58** (15), 9972
38. Diefenbach, J., and Martin, T. P., *Surf. Sci.* (1985) **156**, 234
39. Sunil, K. K., and Jordan, K. D., *J. Phys. Chem.* (1987) **91** (7), 1710
40. Lin, C. C., *et al.*, *ACS Omega* (2021) **6** (28), 17880
41. Wu, J. H., *et al.*, *J. Phys. Chem. C* (2008) **112** (20), 7605